Available online at www.sciencedirect.com
ScienceDirect
Journal of Non-Crystalline Solids 354 (2008) 2144–2148
JOURNAL OF NON-CRYSTALLINE SOLIDS
www.elsevier.com/locate/jnoncrysol

Thermal stability of light-induced defects in hydrogenated amorphous silicon: Effect on defect creation kinetics and role of network microstructure

P. Stradins [a,*], Michio Kondo [b], Akihisa Matsuda [b]

[a] National Renewable Energy Laboratory, CO 80401, USA
[b] National Institute for Advanced Industrial Science and Technology, Tsukuba, Ibaraki 305-8568, Japan

Available online 31 January 2008

Abstract

The kinetics of light-induced defect creation in a-Si:H is studied in early-time limit and as function of pre-existing defects of different thermal stability by electron spin resonance and optical spectroscopy techniques. Both for cw and for laser pulse exposures, the early-time kinetics follows sublinear t^{β} time dependences, similar to the long-time limit. In addition, the overall defect creation rate is not a single function of the total defect number. Instead, it depends on the thermal stability, or annealing energy distribution, of the defects present in the film. Furthermore, creation of the thermally less stable defects is unaffected by the presence of a large number of stable defects introduced by pre-exposure at a higher temperature. These findings question the existing defect creation models. Thermal stability of the light-induced defects depends on the network microstructure, the less stable defects being created in a-Si:H deposited near micro-crystalline transition.
Published by Elsevier B.V.

PACS: 61.43.Dq; 71.23.Cq; 76.30.−v

Keywords: Amorphous semiconductors; Silicon; Chemical vapor deposition; Plasma deposition; Photoinduced effects; Infrared properties; Electron spin resonance; Defects

1. Introduction

The mechanism of light-induced photodegradation of a-Si:H, or Staebler–Wronski effect, still presents a challenge to the field since its discovery in 1977 [1]. The observed sublinear kinetics of Si dangling bond defect creation, $N \sim t^{0.33}$, has been explained by defect creation rate dN/dt that is regulated by the concentration of defects N at a given moment t. The proposed feedback occurs either by photocarrier recombination that is partially redirected through the defect states [2], or by mobile hydrogen being captured into defects instead of forming metastable H pair complexes [3]. Both models finally arrive at a rate equation of type $dN/dt = A/N^2$, from which the sublinear kinetics $N \sim t^{0.33}$ follows in the long-time limit, i.e. when $N(t)$ substantially exceeds the initial defect concentration $N(0)$. At short times when $N(t)/N(0) < 2$, however, the above equation predicts approximately linear kinetics $N \sim t$. The equation also implies that the defect creation rate is a function of a single number, N, the total defect concentration. In the disordered a-Si:H, however, a variety of local environments with different bond angles, lengths, and hydrogen bonding structures, etc. suggests that dN/dt has wide distribution leading to a dispersive behavior that might yield kinetics $\sim t^{\beta}$ already in the short-time limit [4–6]. It has been established that light-induced defects have wide distribution of annealing energies [2], indirectly supporting the above view. These two related topics, short-term kinetics and the creation kinetics dependence on various ways of composing the defect ensemble of concentration N by varying their thermal stability, are addressed in this work.

* Corresponding author.
E-mail address: pauls_stradins@nrel.gov (P. Stradins).

0022-3093/$ - see front matter Published by Elsevier B.V.
doi:10.1016/j.jnoncrysol.2007.09.011

2. Experimental

a-Si:H films were prepared in PECVD reactor at: AIST, Tsukuba, at 100 MHz (VHF) using SiH_4, referred in text as 'VHF' samples; University of Chicago at radio frequency 13.6 MHz ('RF' samples); Pennsylvania State University at 13.6 MHz under $R = 10$ H_2-dilution near the onset of crystallinity ('RF10'). Hot-wire CVD films from NREL ('HW' samples) and expanding thermal plasma CVD films from the University of Eindhoven ('ETP') were also studied. All films were deposited on glass or fused silica at substrate temperature 250–300 °C and were between 1 and 2 μm thick. VHF samples grown under SiH_4 pressure 0.1 Torr, as well as RF and RF10 were of device-grade quality with $\sim 5 \times 10^{15}$ cm^{-3} Si dangling bond defect densities. More defective HW and TEP films exhibited larger values ($>10^{16}$ cm^{-3}). Samples were photodegraded either by filtered cw light at about 0.5 W/cm^2 [6], or by $\lambda = 650$ nm, 6 ns, 1.4 mJ/cm^2 incident laser pulses at 11 Hz repetition rate. Si dangling bond density was measured by electron spin resonance (ESR) with Bruker EMX 6/1 spectrometer, photothermal spectroscopy (PDS), and constant-photocurrent spectroscopy (CPM), with special considerations for high reproducibility and high signal to noise ratio.

3. Results

Fig. 1(A) shows Si dangling bond defect creation kinetics in RF and HW samples under cw light. Subgap absorption α at photon energy 1.3 eV, normalized to its value in the annealed state α_o, was used as measure of defect concentration; $\alpha_{1.3\,eV}$ was measured by CPM and PDS in RF and HW films, respectively. RF samples were exposed at $T = 300$ K (solid circles 1) and 4.2 K (crosses) at photocarrier generation rate $G = 4 \times 10^{21}$ cm^{-3} s^{-1} and measured by CPM at the exposure temperatures [6]. RF films were also exposed at 300 K at 1/14 and 1/40 reduced intensities (solid circles 2 and 3). HW sample was exposed at 300 K at generation rate 10^{22} cm^{-3} s^{-1} and measured by PDS (open circles). Fig. 1(B) shows the same data as in Fig. 1(A), plotted as change in defect density expressed by subgap absorption $\Delta\alpha/\alpha_o = (\alpha - \alpha_o)/\alpha_o$. All the $\Delta\alpha/\alpha_o$ curves exhibit the same power-law dependence on time with exponent between 0.30 and 0.35. One concludes from Fig. 1 that defect creation obeys this sublinear kinetics already at newly created defect densities several times lower than the native defect density. The latter is relatively low in RF sample ($\alpha_o \approx 0.8$ cm^{-1}) but higher in HW film ($\alpha_o \approx 2.5$ cm^{-1}).

In Fig. 2, ETP sample was exposed by laser pulses at $T = 300$ K in two regimes: (1) starting from annealed state (subgap $\alpha_o(1.24\,eV) \approx 4.9$ cm^{-1}) and (2) starting from a strongly pre-degraded state created by laser pulse exposure at elevated $T = 360$ K for 5 h, resulting in high initial defect concentration ($\alpha_o = 24.8$ cm^{-1}). Regimes 1 and 2 are denoted by circles and triangles, respectively. Here, defect

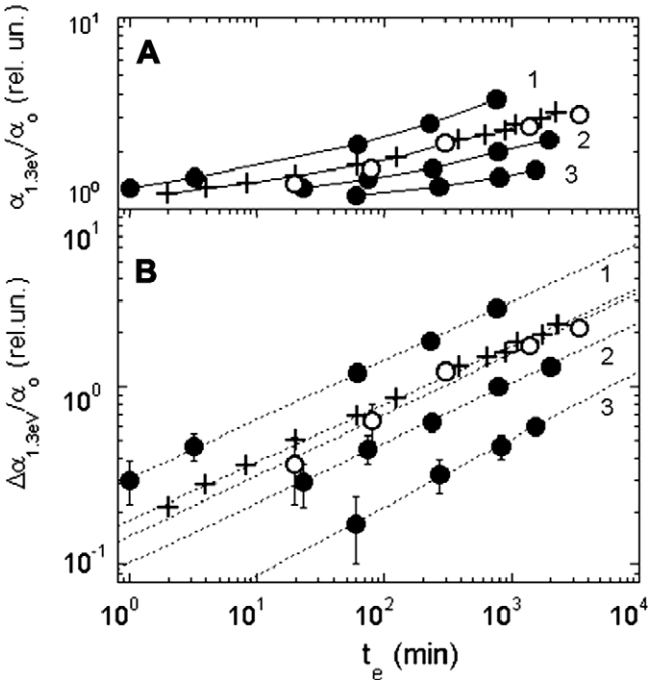

Fig. 1. (A) Increase in subgap absorption α(1.3 eV) due to defect creation in a-Si:H, as function of cw light exposure time t_e. Solid circles: exposure of RF sample at $T = 300$ K at photocarrier generation rate of $G = 4 \times 10^{21}$ cm^{-3} s^{-1} (curve 1), G/14 (curve 2), and G/40 (curve 3). Crosses: exposure of RF sample at 4.2 K at G. Open circles: exposure of HW film at 300 K at 2.5 G. All α(1.3 eV) are normalized by their initial annealed state values α_o. (B) Same data replotted as relative increases of subgap absorption $\Delta\alpha/\alpha_o$. Solid lines are guides to the eye; dotted lines are power-law fits.

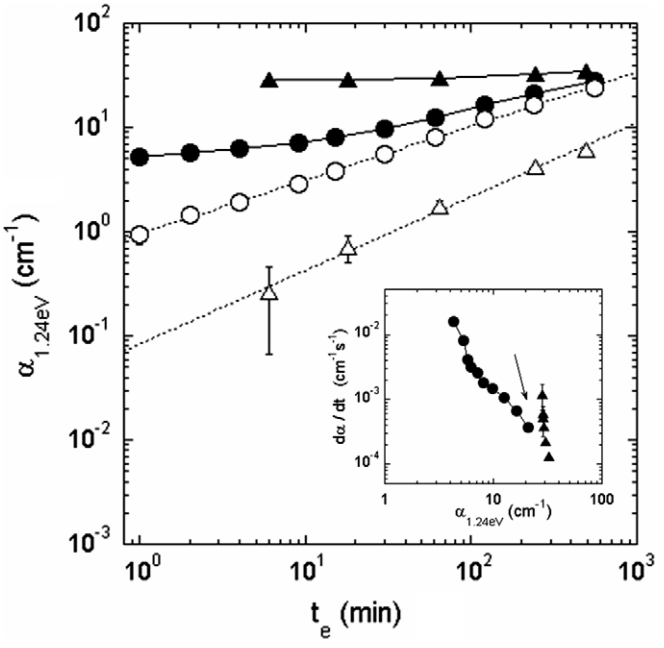

Fig. 2. Changes in subgap absorption α(1.24 eV) due to defect creation by laser pulses at 300 K in ETP sample. Solid circles: α(1.24 eV) as function of exposure time t_e in Regime 1 (starting from annealed state); solid triangles – same, for Regime 2 (starting from a state previously photodegraded at 360 K). Open circles and open triangles: increase in subgap absorption $\Delta\alpha = \alpha(t) - \alpha(0)$ for Regimes 1 and 2, respectively. Solid lines are guides to the eye; dotted lines are power-law fits. Inset: see text.